Journal of Molecular Structure 1020 (2012) 105–111

Contents lists available at SciVerse ScienceDirect

Journal of Molecular Structure

journal homepage: www.elsevier.com/locate/molstruc

Photoionization and dissociation study of p-nitrotoluene: Experimental and theoretical insights

Qiang Zhang [a], Wenzheng Fang [a], Yang Xie [a], Maoqi Cao [a], Yujie Zhao [a], Xiaobin Shan [a], Fuyi Liu [a], Zhenya Wang [b], Liusi Sheng [a,*]

[a] National Synchrotron Radiation Laboratory, School of Nuclear Science and Technology, University of Science and Technology of China, Hefei 230029, People's Republic of China
[b] Laboratory of Environmental Spectroscopy, Anhui Institute of Optics and Fine Mechanics, Chinese Academy of Sciences, Hefei 230031, People's Republic of China

ARTICLE INFO

Article history:
Received 15 January 2012
Received in revised form 24 March 2012
Accepted 24 March 2012
Available online 3 April 2012

Keywords:
P-nitrotoluene
Photoionization
Dissociation
Synchrotron radiation
Ab initio calculations

ABSTRACT

Photoionization and dissociation of p-nitrotoluene in a region of 8.5–16.0 eV have been investigated by tunable vacuum ultraviolet (VUV) synchrotron radiation. The ionization energy (IE) of p-nitrotoluene and the appearance energies (AEs) for major fragments, $C_7H_7O^+$, $C_7H_7^+$, $C_6H_7^+$, $C_6H_5^+$, and $C_5H_5^+$, are determined respectively to be 9.54, 10.95, 11.46, 11.04, 12.45, and 14.25 eV, by measurements of photoionization efficiency (PIE) curves. Five dissociative photoionization channels are proposed: $C_7H_7O^+ + NO$, $C_7H_7^+ + NO_2$, $C_6H_7^+ + NO + CO$, $C_6H_5^+ + NO + CO + H_2$, and $C_5H_5^+ + C_2H_2 + NO_2$. Additionally, the possible formation ways for the major fragments are predicted by *ab initio* calculations at G3B3 level and compared with the experimental results. All of these channels occur via isomerization prior to dissociation except for $C_7H_7^+ + NO_2$. Transition structures and intermediates for those isomerization are also determined in this work.

1. Introduction

P-nitrotoluene belongs to the group of aromatic nitro compounds which have extended use in industrial application, particular in explosives [1]. However, many of these compounds and their transformation products are toxicants [2,3]. P-nitrotoluene is also identified as chemical component of secondary organic aerosol (SOA) from OH-initiated photooxidation of toluene [4] which is mainly originated from vehicle exhaust and industrial emission in the city and plays an important role on formation of SOA [5–7]. Therefore, the understanding of the process for dissociative photoionization of p-nitrotoluene is needed for evaluating the risks involved in aromatic nitro compounds. Moreover, it is also valuable to identify SOA component from photooxidation of toluene and estimate the roles of dissociation fragments in complex aerosol reaction. Although p-nitrotoluene was studied by various experimental or theoretical methods [8–12], the data for photodissociation of p-nitrotoluene is imperfect. As far as we know, AE of $C_5H_5^+$ is only obtained by the electron impact methods and its structure is debatable [12]. Additionally, there is little information about the AEs of $C_6H_7^+$ and $C_6H_5^+$ in the literature until now. Particularly, the mechanism of VUV dissociative photoionization of p-nitrotoluene is still less understood experimentally and theoretically.

In order to determine IE of p-nitrotoluene, AEs for major fragments, and to explore the mechanism for fragmentation pathways, we carried out a study of photoionization and dissociation of p-nitrotoluene using tunable synchrotron VUV in a region of 8.5–16.0 eV. The photoionization mass spectrum of p-nitrotoluene is obtained at photon energy of 15.5 eV. From PIE curves, the IE of p-nitrotoluene and AEs for fragment ions were measured. Furthermore, with the help of *ab initio* calculations, the theoretical IE of p-nitrotoluene, AEs of fragment ions are obtained. In addition, transition states and intermediates involved in the dissociative photoionization channels are also discussed on the basis of theoretical and experimental results.

2. Experimental

The experiments are performed at the Atomic and Molecular Physics Beamline (U14-A) station at the National Synchrotron Radiation Laboratory, Heifei, which has been descried in detail elsewhere [13–15]. In present experiments, the apparatus consists of a molecular beam chamber, a two-stage differential pumping system and a photoionization chamber.

P-nitrotoluene is obtained from J&KCHEMICA (99+%) without further purification. The solid sample is put in a stainless steel tube with the inner diameter of 10 mm and the length of 160 mm. Heater around the tube provides stagnation temperature of 420 K for vaporizing p-nitrotoluene, regulated to within ±1 K. The temperature of the heater is adjusted precisely to vaporize the sample

* Corresponding author. Tel.: +86 0551 3602021; fax: +86 0551 5141078.
E-mail address: lssheng@ustc.edu.cn (L. Sheng).

0022-2860/$ - see front matter © 2012 Elsevier B.V. All rights reserved.
http://dx.doi.org/10.1016/j.molstruc.2012.03.059

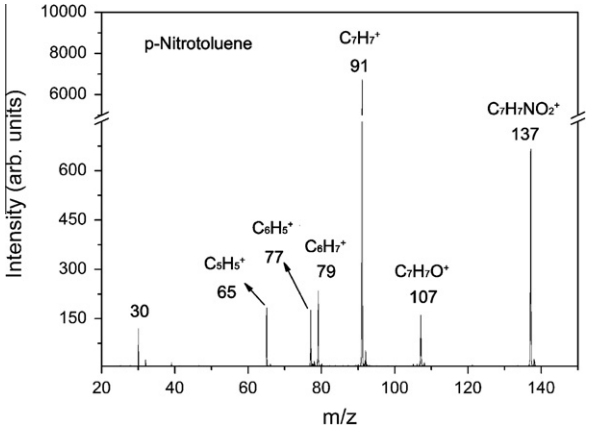

Fig. 1. Photoionization mass spectrum of p-nitrotoluene at 15.5 eV.

and prevents them from dissociation. The p-nitrotoluene vapor carried by Ar at 0.05 MPa is expanded into the ionization chamber through a nozzle and two skimmers to form molecular beam. The monochromatic VUV synchrotron radiation from the electron storage ring intersects perpendicularly with the beam to ionize p-nitrotoluene molecule in the photoionization chamber. The ions produced here are analyzed with the reflectron time-of-flight mass spectrometer mounted in a direction perpendicular to the plane defined by molecular and photon beam. A microchannel plate (MCP) detector serves for the collection and detection of the ions formed in ionization region. Signals from the detected ions are counted with a multiscaler P7888 counter (FAST Comtec, Germany) after they are amplified with preamplifier VT120C (EG&G, ORTEC) and transferred to a computer for further processing.

The photoionization mass spectrum of p-nitrotoluene can be obtained when it's excited by using a fixed photon energy above its ionization threshold. The PIE curves are measured while the monochromator is scanned from 8.5 to 16.0 eV with the energy increment of 30 meV. To normalize the ion signals, the photon intensity is monitored simultaneously with a silicon photodiode (SXUV-100, International Radiation Detectors, Inc.). In the study, we use the rare-gas (Ar) harmonic filter to reduce higher-order harmonics, and the pressure of the gas filter is about 665 Pa with the efficiency of above 99.9 % [14].

3. Theoretical calculation

In the theoretical study, all the geometry optimizations of the reactants, transition states, intermediates, and products are done at the B3LYP level with 6-31G (d) basis sets, and harmonic vibrational frequencies are also computed analytically at the same level in order to characterize the optimized geometries as potential minima or saddle points. The relative energies are obtained at the G3B3 level based on the optimized geometries at the B3LYP/6-31G (d) level. The structures of transition states and intermediates for dissociative photoionization channels are also identified in this study. All *ab initio* calculations, performed with the GAUSSIAN 09 program, are carried out on the Supercomputing Center of University of Science and Technology of China.

4. Results and discussion

4.1. Results

The photoionization mass spectrum of p-nitrotoluene at 15.5 eV is shown in Fig. 1. In the graph, the parent ion and the main fragment ions, $C_7H_7O^+$ (*m/z* 107), $C_7H_7^+$ (*m/z* 91), $C_6H_7^+$ (*m/z* 79), $C_6H_5^+$ (*m/z* 77), and $C_5H_5^+$ (*m/z* 65) can be distinguished clearly. Moreover, the peak corresponding to fragment $C_7H_7^+$ has the strongest intensity, far more than the intensities of other peaks, suggesting the direct dissociation for parent ion to $C_7H_7^+$ and NO_2 dominating the dissociation at the photon energy of 15.5 eV. The intensities of peaks corresponding to other fragment ions, $C_7H_7O^+$, $C_6H_7^+$, $C_6H_5^+$, and $C_5H_5^+$, are almost the same.

The PIE curves of p-nitrotoluene and fragment ions, $C_7H_7O^+$, $C_7H_7^+$, $C_6H_7^+$, $C_6H_5^+$, and $C_5H_5^+$ are shown in Fig. 2a and f respectively. The IE of parent ion and the AEs of fragment ions can be obtained directly by scanning the photon energy of the monochromator. After subtracting background and normalizing to the photon flux, we derive IE and AEs of 9.54, 10.95, 11.46, 11.04, 12.45, and 14.25 eV for $C_7H_7NO_2^+$, $C_7H_7O^+$, $C_7H_7^+$, $C_6H_7^+$, $C_6H_5^+$, and $C_5H_5^+$ according the first discernible onset over the baseline by using nonlinear least squares fit. For instance, the IE of $C_7H_7NO_2^+$ is derived from the first detection of ion signal and is 9.54 eV. This value is well in agreement with quantum chemical calculations result 9.56 eV and it's also close to other experimental values as listed in Table 1. Table 1 lists the IE of parent ion and the AEs of the main fragment ions involved in dissociative photoionization of p-nitro-

Table 1
Experimental, theoretical, and literature values of the IE, AE, and dissociation energy (Ed) or reaction barriers V(G3B3) of possible dissociative channels. Experimental method codes used in table: Photoion–photoelectron coincidence spectroscopy (PIPECO), Photoelectron spectroscopy (PE), Electron impact techniques (EI), Photoionization mass spectrometry (PI).

Ions	IE or AE (G3B3) (eV)	IE or AE (Exp.) (eV)	Ref.	Ref. No.	Possible dissociation channels	Ed (G3B3) (eV)	V (G3B3) (eV)	Ed (Exp.) (eV)
$C_7H_7NO_2^+$	9.56	9.54	9.46 ± 0.05(PIPECO)	[8]				
			9.54 ± 0.015(PE)	[16]				
			9.56 (EI)	[10]				
			9.5 ± 0.1 (EI)	[17]				
			9.76 ± 0.05 (EI)	[18]				
$C_7H_7O^+$	9.01	10.95	10.91 ± 0.05(PI)	[19]	$C_7H_7O^+ + NO$	−0.55	1.26	1.41
			10.3 ± 0.1 (EI)	[17]				
$C_7H_7^+$	11.39	11.46	11.3 ± 0.1 (PI)	[19]	$C_7H_7^+ + NO_2$	1.83		1.92
			11.15(PIPECO)	[8]				
			12.3 ± 0.3 (EI)	[20]				
			11.8 ± 0.1 (EI)	[17]				
$C_6H_7^+$	9.78	11.04	–		$C_6H_7^+ + NO + CO$	0.22	1.26	1.50
$C_6H_5^+$	11.16	12.45	–		$C_6H_5^+ + NO + CO + H_2$	1.60	3.09	2.91
$C_5H_5^+$	13.81	14.25	14.9 ± 0.2 (EI)	[12]	$C_5H_5^+ + NO_2 + C_2H_2$	4.25	4.62	4.71

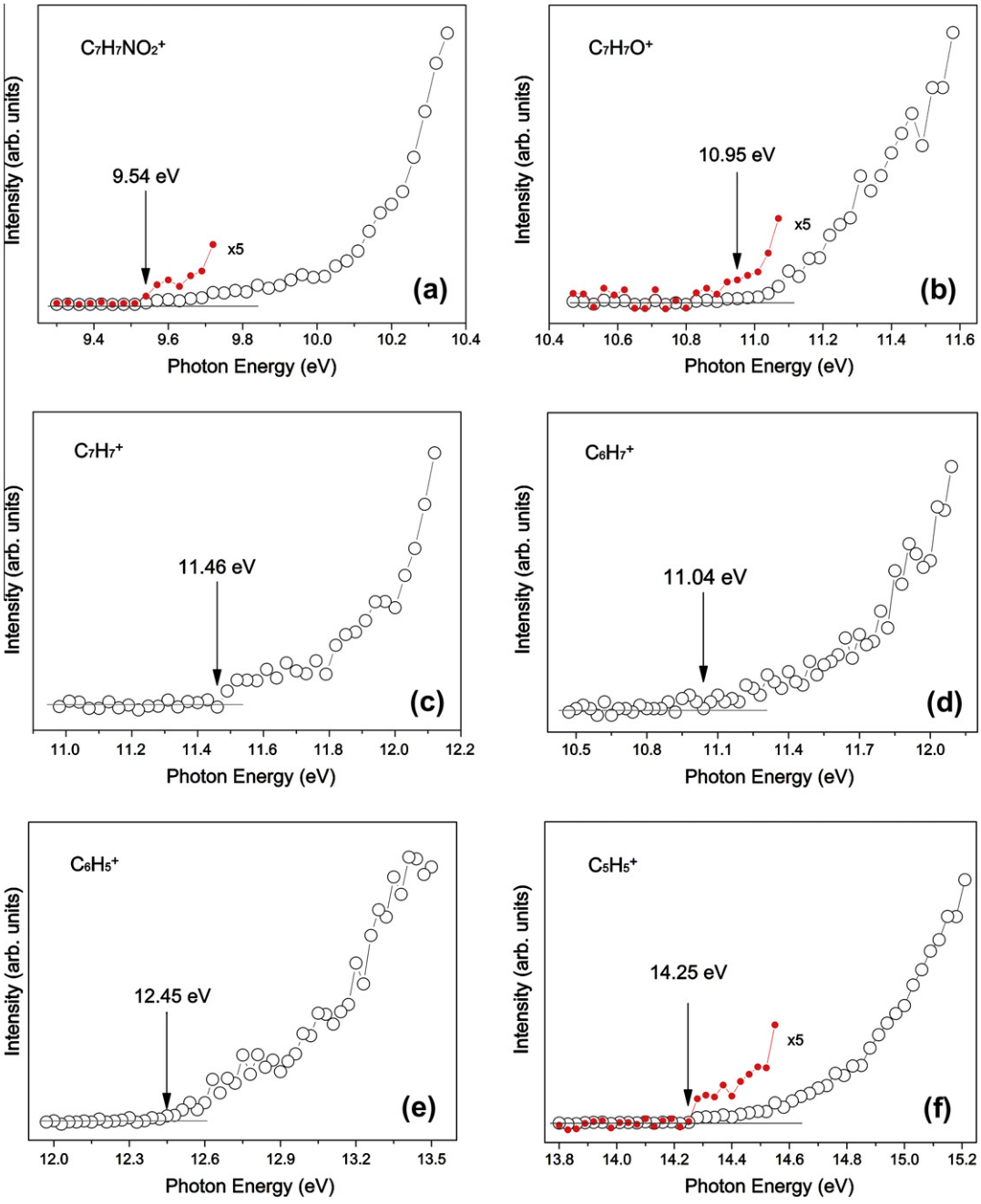

Fig. 2. PIE curves for $C_7H_7NO_2^+$ (a), $C_7H_7O^+$ (b), $C_7H_7^+$ (c), $C_6H_7^+$ (d), $C_6H_5^+$ (e), and $C_5H_5^+$ (f). The signals of $C_7H_7NO_2^+$, $C_7H_7O^+$ and $C_5H_5^+$, amplified with a factor of 5 at the lower energies respectively, are shown in the red in (a and b and f).

toluene. For AEs of $C_6H_7^+$ and $C_6H_5^+$, they haven't been recorded in the US National Institute of Standards and Technology (NIST) database and are determined in our work. The dissociation energies and the possible dissociation channels are also listed in Table 1. The dissociation energy (Ed) is calculated by subtracting IE of parent molecule from AE of relative fragment ion. In the case of $C_7H_7NO_2^+ - NO$, the IE of $C_7H_7NO_2^+$ is 9.54 eV and the AE of $C_7H_7O^+$ is 10.95 eV. Consequently, the experimental Ed is 1.41 eV.

4.2. Dissociation mechanisms

The fragments of p-nitrotoluene in the dissociative photoionization have already been discussed elsewhere [8,12,17,21–24]. Fragmentation channels also have been described as follows: $C_7H_7O^+ + NO$, $C_7H_7^+ + NO_2$, $C_6H_7^+ + NO + CO$, $C_6H_5^+ + NO + CO + H_2$, $C_5H_5^+ + NO_2 + C_2H_2$. However, the detailed mechanisms of the fragmentation pathways have not been clarified. Additionally, AE of $C_5H_5^+$ is only obtained by the electron impact methods and there is little information about the AEs of $C_6H_7^+$ and $C_6H_5^+$ in the literature until now. In our work, the parent ion can be generated directly by a single-photon ionization of the VUV synchrotron radiation. The dissociation reactions occur as the photon energy rises. The dissociative mechanisms of $C_7H_7NO_2^+$ are discussed based on our experimental, theoretical and previous studies [8–12]. These dissociative channels are shown in Figs. 3–5 respectively. In addition, the detailed information on the geometries and energies of the optimized reactants, transition states, intermediates and products are also shown in Figs. 6–8 and Table 2. At the

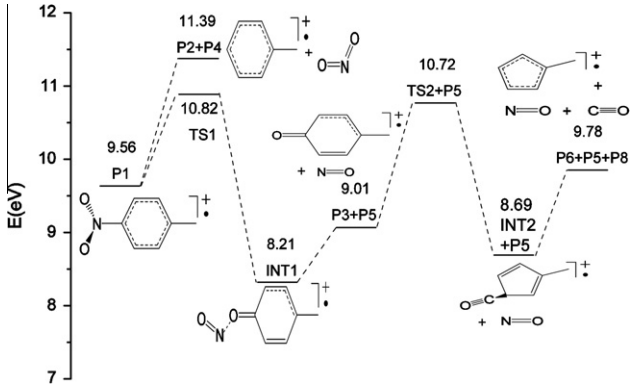

Fig. 3. The dissociation channels for p-nitrotoluene cation to producing fragment ions, $C_7H_7^+$(P2), $C_7H_7O^+$(P3) and $C_6H_7^+$(P6), calculated at the G3B3 level. The energy of neutral p-nitrotoluene is defined to be zero.

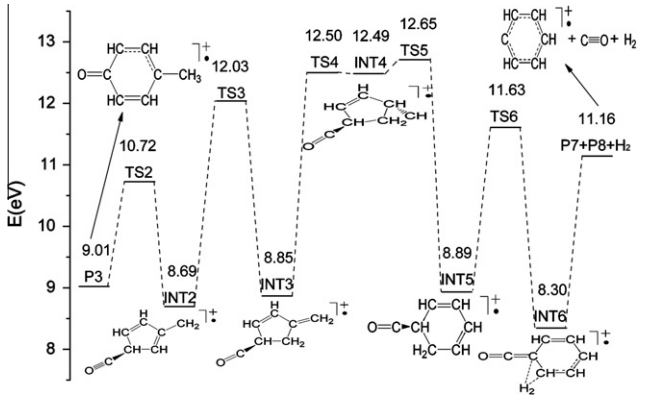

Fig. 4. The dissociation channel for p-nitrotoluene cation to producing fragment ion $C_6H_5^+$, calculated at the G3B3 level. The energies of the products, transition states and intermediates which marked in the graph are obtained by the sum of the energy of the corresponding species and the energy of NO, minus the energy of neutral p-nitrotoluene.

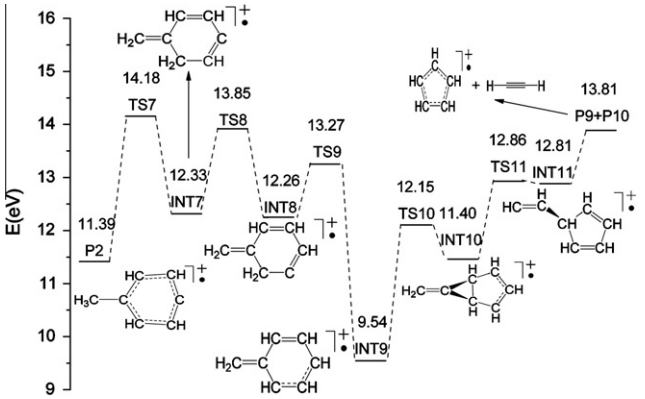

Fig. 5. The dissociation channel for p-nitrotoluene cation to producing fragment ion $C_5H_5^+$, calculated at the G3B3 level. The energies of the products, transition states and intermediates which marked in the graph are obtained by the sum of the energy of the corresponding species and the energy of NO2, minus the energy of neutral p-nitrotoluene.

Table 2
Calculated energies at the G3B3 level.

Species	E_0 (G3B3/hartree)	Species	E_0 (G3B3/hartree)
$C_7H_7NO_2$ (R1)	−475.758530	$C_7H_7NO_2^+$(P1)	−475.407209
$C_7H_7^+$ (P2)	−270.355953	$C_7H_7O^+$ (P3)	−345.591345
NO_2 (P4)	−204.984022	NO (P5)	−129.836250
$C_6H_7^+$ (P6)	−232.292970	$C_6H_5^+$ (P7)	−231.074753
CO (P8)	−113.269969	$C_5H_5^+$ (P9)	−192.988240
C_2H_2 (P10)	−77.278697	H_2	−1.167475
TS1	−475.361045	INT1	−475.456715
TS2	−345.528495	INT2	−345.602853
TS3	−345.480072	INT3	−345.597221
TS4	−345.462798	INT4	−345.463060
TS5	−345.457247	INT5	−345.595663
TS6	−345.494965	INT6	−345.617173
TS7	−270.253255	INT7	−270.321367
TS8	−270.265351	INT8	−270.324007
TS9	−270.286968	INT9	−270.423980
TS10	−270.328047	INT10	−270.355732
TS11	−270.301915	INT11	−270.303889

same time, standard heats of formation (kJ/mol) of species involved in dissociative photoionization of p-nitrotoluene are listed in Table 3. Calculation method of the heat of formation is reported in Ref. [12] and here we also neglect the excess energies of the fragments.

Generally, there are two types of mechanisms for dissociation: directly simple bond cleavage or indirect bond cleavage via transition states and intermediates. The $C_7H_7^+$ ions are formed by loss of NO_2 from the molecular ions under photoionization condition. This is one-step dissociation process with no distinct transition states as reported previously [17]. The AE of experimental 11.46 eV is quite consistent with the theoretical value 11.39 eV. The heat of formation for $C_7H_7^+$ is 1103.5 kJ mol^{-1} at present work, which is roughly the same as Bear's [8] work 1074 kJ mol^{-1} (Table 3).

The $C_7H_7O^+$ ions are produced by elimination NO from parent ions. A metastable ion analysis by Beynon et al. [21] suggested that loss of NO from the molecular ions of aromatic nitro compounds occurs via two unimolecular processes which appear to be in competition with each other: one is a three-centered cyclic transition state with the formation of the aryloxy cation; the other is oxygen rearrangement to the ortho position. Talking about p-nitrotoluene molecule, one process involves an oxygen transfer to the C4 (as marked in Fig. 8) and results in the formation of $C_7H_7O^+$, the other process was believed to involve an oxygen transfer to the ortho carbon C3 or C5. However, both the evidences from previous experiments [17,22] and present results prefer the former interpretation. The structure of the transition state TS1 and product P3 are shown in Figs. 6 and 8, respectively. The N–C bond breaks gradually and O–C bond begins forming in the transition state. The length of the bonds for N–C and O–C are 1.578, 1.630 Å of TS1. Detailed formation pathway of $C_7H_7O^+$ with potential energy diagram is depicted in Fig. 3. The $C_7H_7O^+$ ions are formed via transition state TS1 with an energy barrier of 1.26 eV, which is 0.15 eV below the experimental Ed.

The $C_7H_7O^+$ ions will decompose to $C_6H_7^+$ and CO or $C_6H_5^+$, CO, and H_2 in some condition which have been reported previously [22]. $C_7H_7O^+$ isomerizes into transition state TS2 (Fig. 6) for elimination CO by the C4–C5 and C4–C3 bonds cleavage to form $C_6H_7^+$. The CO loss reaction channel is shown in Fig. 3. This reaction barrier is also determined by TS1, which is 0.24 eV below the experimental Ed. From the calculation results, $C_6H_7^+$ should be along with the presence of $C_7H_7O^+$. Our experimental AEs with difference about 0.09 eV between the $C_7H_7O^+$ and $C_6H_7^+$ also reasonably verify the theoretical predictions. However, the process for $C_6H_5^+$ is somewhat complicated as shown in Fig. 4. First, the product $C_7H_7O^+$ isomerizes into TS2, then two hydrogens of methyl transfer to C2 and C1 respectively. Then after ring expanding, INT6 subsequently forms $C_6H_5^+$, CO, and H_2. The reaction barrier for this dissociation

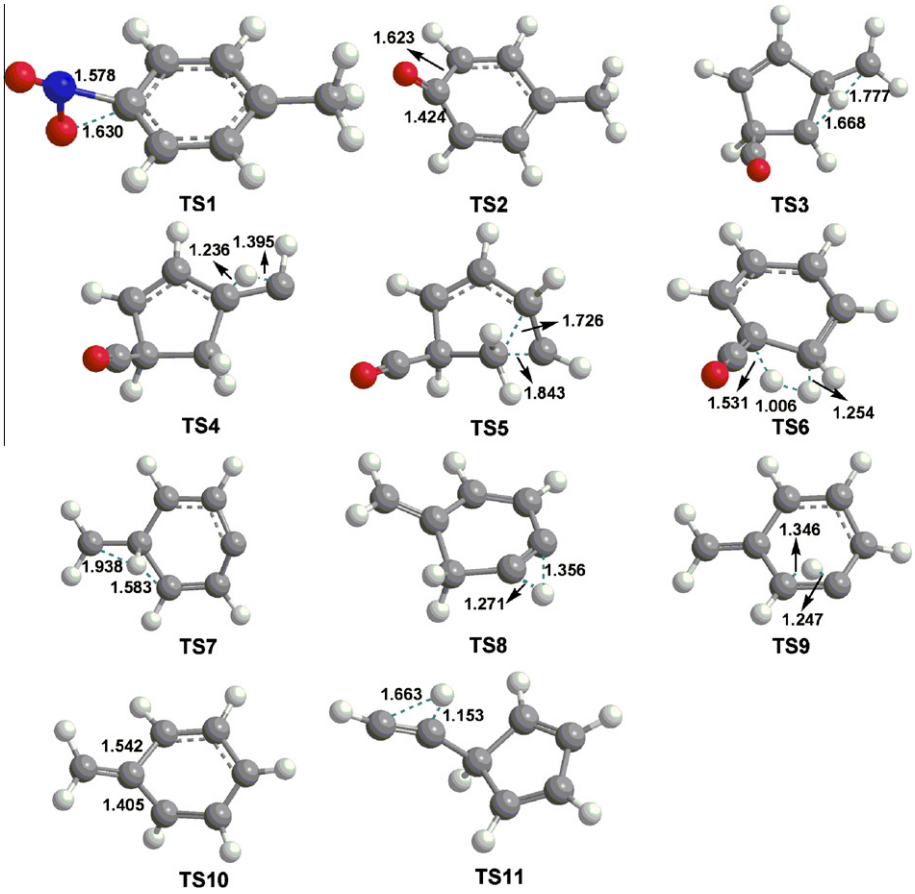

Fig. 6. The geometries of the transition states at the G3B3 level (bond length unit: Å).

Table 3
Standard heats of formation (kJ mol^{-1}) of species involved in dissociative photoionization of p-nitrotoluene.

Neutral	$\Delta H^o_{f,298}$	Cation	$\Delta H^o_{f,298}$
$C_7H_7NO_2$	30.9[g]	$C_7H_7NO_2^+$	951.4[a], 944[b], 761[e]
NO_2	33.1[h]	$C_7H_7O^+$	1054.3[a], 803[e]
NO	90.3[h]	$C_7H_7^+$	1103.5[a], 1074[b], 1192.4[c]
CO	−110.5[h]	$C_6H_7^+$	836.3.8[a], 854[e]
C_2H_2	226.7[h]	$C_6H_5^+$	1031.4[a], 1129[f]
H_2	0[i]	$C_5H_5^+$	1146.0[a], 1217.5[d]

[a] This work.
[b] Ref. [8].
[c] Ref. [20].
[d] Ref. [12].
[e] Ref. [22] ($\Delta H^o_{f,298}$ ($C_7H_7NO_2$) = −41.4 kJ mol^{-1}).
[f] Ref. [23].
[g] Ref. [26].
[h] Ref. [27].
[i] Ref. [28].

is 3.09 eV, 0.18 eV greater than the experimental Ed. All the structures and bond lengths of the products, transition states and intermediates involved in this process are shown in Figs. 6–8.

It is well known that the $C_7H_7^+$ ions can decompose into the $C_5H_5^+$ by losing C_2H_2 [12]. However, the structure for $C_5H_5^+$ is controversial. Occolowitz and White [25] have concluded the geometry of $C_5H_5^+$ ion can be identified as chain structure or ring structure. In our calculation, the results favor the latter one. Detailed pathway is described in Fig. 5. When the photon energy is above 14.18 eV, the product ion $C_7H_7^+$ will go through isomerization before decomposing into $C_5H_5^+$. In this process, two hydrogen atoms on methyl of product P2 (Fig. 8) will be migrant. After several transfers for hydrogens as shown in Fig. 5, with a hydrogen on each carbon, hydrogen on C7 transfers to C1 and C1−C6 bond cleavage, C_2H_2 subsequently loss and $C_5H_5^+$ ion is formed. The reaction barrier for producing the $C_5H_5^+$ is 4.62 eV at the G3B3 level and is in good agreement with the experimental result 4.71 eV. The heat of formation for $C_5H_5^+$ is 1146 kJ mol^{-1} at present work, which is in reasonable agreement with Tajima and Tsuchiya's [12] work 1217.5 kJ mol^{-1} (Table 3).

5. Conclusions

IE of p-nitrotoluene and AEs of dissociation fragment ions $C_7H_7O^+$, $C_7H_7^+$, $C_6H_7^+$, $C_6H_5^+$, and $C_5H_5^+$ have been determined to be 9.54, 10.95, 11.46, 11.04, 12.45, and 14.25 eV, respectively, utilizing tunable VUV synchrotron radiation in conjunction with reflectron time-of-flight mass spectrometry. The experimental dissociation energies are in good agreement with theoretical results. Detailed information of fragmentation pathways are also discussed, especially for $C_6H_7^+$ and $C_5H_5^+$. Geometries and energies of fragment ions, transition states and intermediates involving in the dissociative photoionization channels have also been determined by theoretical calculation. Meanwhile, combining with the known information of thermochemical parameters, standard heat of formation for fragment ions are derived and helpful to understand the fragmentation pathways.

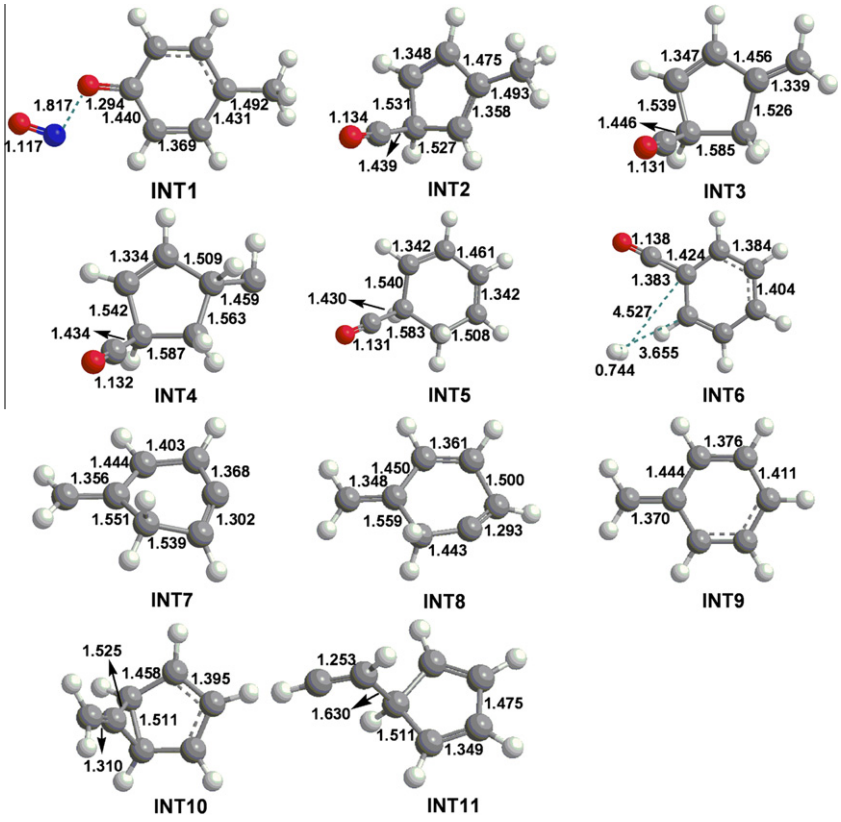

Fig. 7. The geometries of the reactant intermediates at the G3B3 level (bond length unit: Å).

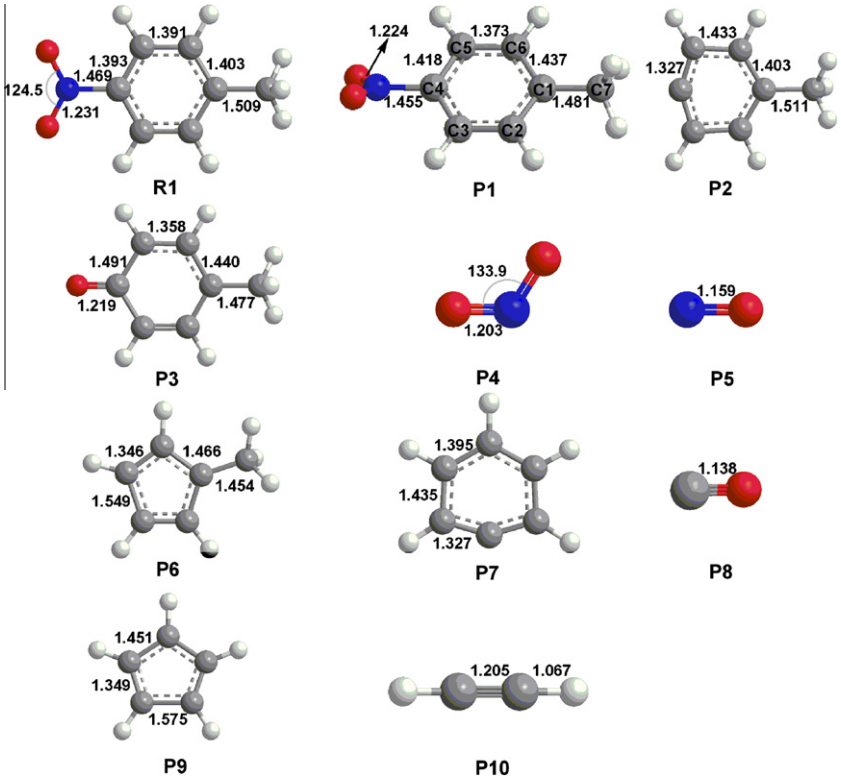

Fig. 8. The geometries of the neutral p-nitrotoluene, its cation and its fragments (ions and neutrals) at the G3B3 level (bond length unit: Å).

Acknowledgements

The authors thank the Knowledge Innovation Foundation of the Chinese Academy of Sciences (KJCX2-YW-N07) and the National Natural Science Foundation of China (Nos. 11075165, 10874167, and 10675112) for support.

References

[1] T.B. Brill, K.J. James, Chem. Rev. 93 (1993) 2667.
[2] H. Tokiwa, Y. Ohnishi, Crit. Rev. Toxicol. 17 (1986) 23.
[3] K.E. Anderson, G.J. Hammons, F.F. Kadlubar, J.D. Potter, K.R. Kaderlik, K.F. Ilett, R.F. Minchin, C.H. Teitel, H.C. Chou, M.V. Martin, F.P. Guengerich, G.W. Barone, N.P. Lang, L.A. Peterson, Carcinogenesis 18 (1997) 1085.
[4] W.Z. Fang, L. Gong, X.B. Shan, F.Y. Liu, Z.Y. Wang, L.S. Sheng, Anal. Chem. 83 (2011) 9024.
[5] M.S. Jang, R.M. Kamens, Environ. Sci. Technol. 35 (2001) 3626.
[6] I. Suh, R.Y. Zhang, L.T. Molina, M.J. Molina, J. Am. Chem. Soc. 125 (2003) 12655.
[7] R. Atkinson, Atmos. Environ. 34 (2000) 2063.
[8] T. Baer, J.C. Morrow, J.D. Shao, S. Olesik, J. Am. Chem. Soc. 110 (1988) 5633.
[9] R. Egdell, J.C. Green, C.N.C. Rao, Chem. Phys. Lett. 33 (1975) 600.
[10] R.A.W. Johnstone, F.A. Mellon, Faraday Trans. 2 (69) (1973) 36.
[11] T. Kobayashi, S. Nagakura, Bull. Chem. Soc. Jpn 47 (1974) 2563.
[12] S. Tajima, T. Tsuchiya, Bull. Chem. Soc. Jpn. 46 (1973) 3291.
[13] S.S. Wang, R.H. Kong, X.B. Shan, Y.W. Zhang, L.S. Sheng, Z.Y. Wang, L.Q. Hao, S.K. Zhou, J. Synchrotron. Radiat. 13 (2006) 415.
[14] W.Z. Fang, G. Lei, X.B. Shan, F.Y. Liu, Z.Y. Wang, L.S. Sheng, J. Electron Spectrosc, Relat. Phenom. 184 (2011) 129.
[15] W.Z. Fang, G. Lei, Q. Zhang, X.B. Shan, F.Y. Liu, Z.Y. Wang, L.S. Sheng, J. Chem. Phys. 134 (2011) 174306.
[16] T. Kobayashi, S. Nagakura, Chem. Lett. 10 (1972) 903.
[17] P. Brown, Org. Mass Spectrom. 4 (1970) 533.
[18] A. Buchs, Helv. Chim. Acta. 53 (1970) 2026.
[19] V.M. Matyuk, V.K. Potapov, A.L. Prokhoda, Russ. J. Phys. Chem. 53 (1979) 538.
[20] F.W. McLafferty, J. Winkler, J. Am. Chem. Soc. 96 (1974) 5182.
[21] J.H. Beynon, M. Bertrand, R.G. Cooks, J. Am. Chem. Soc. 95 (1973) 1739.
[22] D.H. Russell, B.S. Freiser, E.H. McBay, D.C. Canada, Org. Mass Spectrom. 18 (1983) 474.
[23] C.J. Cassady, B.S. Freiser, D.H. Russell, Org. Mass Spectrom. 18 (1983) 378.
[24] E.L. Eliel, J.D. McCollum, S. Meyerson, P.N. Rylander, J. Am. Chem. Soc. 83 (1961) 2481.
[25] J.L. Occolowitz, G.L. White, Aust. J. Chem. 21 (1968) 997.
[26] C. Lenchitz, R.W. Velicky, G. Silvestro, L.P. Schlosberg, J. Chem. Thermodyn. 3 (1971) 689.
[27] M.W. Chase Jr Jr., J. Phys. Chem. Ref. Data Monograph 9 (1998) 1.
[28] S.G. Lias, J.E. Bartmess, J.F. Liebman, J.L. Holmes, R.D. Levin, W.G. Mallard, J. Phys. Chem. Ref. Data. 17 (1988) 1.